Combining Shape Analysis and Texture Pattern for Palmprint Recognition

Raouia Mokni, Hassen Drira, Monji Kherallah

HAL Id: hal-01532152
https://hal.science/hal-01532152

Submitted on 2 Jun 2017

Combining Shape Analysis and Texture Pattern for Palmprint Recognition

Raouia Mokni · Hassen Drira, · Monji Kherallah

Abstract we propose an efficient method for principal line extraction from the palmprint and geometric framework for analyzing their shapes. This representation, along with the elastic Riemannian metric, seems natural for measuring principal line deformations and is robust to challenges such as orientation variation and re-parameterization due to pose variation and missing part, respectively. The palmprint texture is investigated using the fractal analysis; thus the resulting features are fused with the principal line features. This framework is shown to be promising from both empirical and theoretical perspectives. In terms of empirical evaluation, our results match or improve the state-of-the-art methods on three prominent palmprint datasets: PolyU, CASIA, and IIT-Delhi, each posing a different type of challenge. From a theoretical perspective, this framework allows fusing texture analysis and shape analysis.

Raouia Mokni
Faculty of Economics and Management of Sfax (FSEGS), University of Sfax, Tunisia
E-mail: raouia.mokni@gmail.com

Hassen Drira
The Institut Mines-Télécom/Télécom Lille; CRIStAL (UMR CNRS 9189), France. E-mail: hassen.drira@telecom-lille.fr

Monji Kherallah
Faculty of Sciences of Sfax, University of Sfax, Tunisia. E-mail: Monji.kheralllah@enis.rnu.tn

1 Introduction and related work

1.1 Introduction

The broad proliferation of information technology has aroused the real need for a reliable and easy automatic mechanism to identify individuals. Conventional means based on passwords and/or magnetic cards present a some limitations, as they may be stolen or compromised. In contrast, biometrics has been emerging and developing as a new and effective identification technology counterpassing these inconveniences. By human biometrics, we mean the use of physiological characteristics, of human body parts and their appearances, to identify individual human beings in the course of their daily activities. The biometrics researchers have focused on body parts and images that try to minimize the variability within class (subjects) and maximize it across classes. Palmprint has drawn considerable attention of many researchers thanks to its rich, stable and unique features like principal lines, wrinkles, ridges, minutiae points, singular points and texture. Some of these features, such as the minutiae and the singular points, need a high resolution palmprint image; at least 400 dpi. They are suitable for Medico-legal applications as the identification of criminals where the acquisition is done by the ink or the use of the latent prints for offline recognition. On the other hand, low resolution Palmprint images, less than 150 dpi, are suitable for civil and commercial applications like access control and real-time authentication where the recognition is done online. Although the minutiae and the singular points can not be revealed in low resolution images, principal lines, wrinkles, ridges and texture are easily extracted from these images. A reliable palmprint identification system is able to recognize the persons using the majority of the available information. One of the reliable ways to achieve a higher level of performance is to combine the palmprint modality with other modalities (multimodal or inter-modal systems) or fuse several descriptors for a single modalality (intra-modal systems) which have shown promising results in the palmprint identification [26, 40, 25, 7].

1.2 Related work

In this section, we provide an overview of the related work methods for palmprint identification systems. The later can be considered as the current and future key for solving security problems due to their several advantages, such as the low-resolution imaging with the low-cost capturing devices (cheaper devices), the higher level of security, difficulty to forge and user friendly interface, etc.

So far, these already existing proposed systems can be subdivided into three popular categories mainly on the basis of extracted features.
(1) ***Texture-pattern-based-approaches*** are the global approaches which have been widely-studied. The task of recognizing the individuals by the tex-

ture of their palmprint has been approached in several ways, which leads to successful varying levels. Several approaches have been suggested to describe the texture of palmprint in recent years. Among these, we can mention those of which Hammami et al. [17] proposed an approach based on dividing the whole images into sub-images and applying the LBP operator to analyze the textures for each sub-image. Then, these authors investigate the SFFS algorithm in order to select the pertinent features of the palmprint texture. In order to determine the identity of a person, a chi-square X^2 statistic is used based on calculating the Chi-square distance between the image test and all the images. They evaluated their approach on two datasets with several challenges in terms of variations of orientation, position and illumination in capturing palmprint images. In [37], wang et al. described a novel algorithm for palmprint texture recognition based on combining the 2D Gabor wavelets and Pulse Coupled Neural Network (PCNN). These authors decomposed the palmprint images by 2D Gabor wavelets. Then, they employed the PCNN to decompose each resulting Gabor sub-band into a set of binary images, followed by a Support Vector Machines (SVM) classifier for classification. A roughly similar idea is proposed by khalifa et al. [23] that used the Gabor filters for feature texture extraction, treating the SVM as a classifier for palmprint identification. Moreover, the authors described two other methods to analyze the palmprint texture like the Co-occurrence Matrix (CM) and the Discrete Wavelet Transform (DWT) and used yet the SVM in classification phase. Charfi et al. [7] presented a new identification system focusing on the extraction of the palmprint texture using the Scale Invariant Feature Transform (SIFT). In [21], Jawsal et al. employed 2D Gabor filter to describe the palmprint texture information and used subspace methods for dimension reduction like PCA and LDA. Then, the Euclidean distance is used for the matching phase.

Likewise, the fractal geometry theory is one of the most efficient achievements in mathematics in the 20th century as it contains several methods which are among the earliest successful methods used to analyze the image texture in the pattern recognition and the image processing fields [32]. In fact, such methods have been reliably applied to extract the behavioral features like handwriting [6] and signature [41] in the literature. These obtained results are very promising and have given high performance in the behavioral biometric recognition systems.

(2) **Line-based-approaches** group the structural approaches which are based specifically on principal lines [38], wrinkles [8], ridge and feature point [13]. Numerous approaches have been proposed to extract the principal lines of the palmprint. In particular, Tunkpien et al. [36] proposed an approach to extract the principal lines of palmprint based on an average filter and magnitude gradient. Then, they used the morphological operators for smoothing the principal line contours. In [4], the principal line detection is performed by six steps which are normalization, median filtering, average filters, grayscale bottom-hat filtering, combinations of bottom-hat operations, binarization and post processing. Khan et al. [24] proposed another algorithm which uses Niblack binarization, morphological operation and thinning to extract the principal

lines. Then, they detected the endpoints of the lines and created a connection between them. Finally, the authors exploited the quantitative features from the triangle of Delaunay Triangulation in order to identify the persons. Han et al. [18] detected the palm lines by the Sobel and morphological operations. Wu et al. [38] extracted principal lines using canny edge algorithm. The feature vector is determined by the magnitude and orientation of the gradient for each edge point. Then, the fuzzy energy of each direction was calculated in order to generate this feature vector.

Unfortunately, the previously proposed works could not explicitly and clearly extract the principal lines and achieve high recognition rates. Besides, there has not been any suggestion to determine the shape for each detected line with the existing challenge, such as illumination, direction and position variations which include the contraction and stretching of the principal lines, during the palmprint collection.

(3) ***Intra-modal-based-approaches*** are the recently proposed approaches which are based on the information fusion technologies that have shown promising results in palmprint identification. Several approaches utilize the fusion technique based on multi-descriptors to define the multiple features that are eventually used in identification. In fact, Kumar et al. [27] provided an approach based on combining the various representations which represent the multi-features such as Gabor-based texture feature, line feature and PCA feature. Similarly, Krichneswari et al. [25] proposed an intra-modal feature fusion system based on extracting multiple features like Gabor texture and Line features for palmprint recognition. Then, the authors used the Particle Swarm Optimization (PSO) and Principal Component Analysis (PCA) to reduce the feature vector and matched them with stored template using NN classifier. Likewise, Luo et al. [28] used the LBP-structure descriptors and the Local Line Directional Pattern (LLDP) with different parameters to extract the texture and the line space, respectively. In [40], the authors proposed a new hierarchical method for palmprint recognition based on generating the major principal lines with a probability distribution template and applying the Dual Tree Complex Wavelet (DTCW) to extract the texture feature of palmprint image. In [26], the authors investigated a novel method using nonlinear rank level combination of multiple palmprint feature representations which are principal lines, Eigen Palm and Gabor filter texture. Hu et al.[19] proposed a new algorithm based on fusing three important features of palmprint, such as texture feature, principal lines and appearance feature applying 2D Gabor filter, MFRAT and ODLPP, respectively.

The intra-modal based approaches conclude that using multi-features yields better results than using a single feature for a single biometric modality (uni-modal).

2 Overview of the proposed approach

In this paper, we investigate an intra-model palmprint identification system. The technique consists in efficiently combining the principal line shape analysis and the texture pattern analysis to make the system more robust. The overview of the shape analysis approach and the fractal based method are depicted in Fig.1.a and Fig.1.b respectively. The principal lines are extracted as three types of curves (C_1, C_2 and C_3) based on Steerable filter and Hysteresis thresholding as illustrated in Fig.1.a The shape analysis framework is then applied between the extracted curves. Representatives for each person Per_j are calculated using training data for each type of curve (C_1, C_2 and C_3), where j={1,2,...,k}. These representatives are the intrinsic means provided by the shape analysis framework, of all curves belonging to the same person Per_j and same curve type C_i. The feature vector for a given curve β of type C_i is calculated based on the distance between β and all the means corresponding to the same type C_i. A probe image is considered as three curves of different classes.

The texture information is next investigated based on fractal analysis as illustrated in Fig.1.b. The texture pattern information is extracted based on the fractal approach on calculating the fractal dimension obtained by the box counting method. Furthermore, we combine the relevant information of the different obtained features from the principal line shape and the texture pattern to increase the system accuracy. Finally, the palmprint recognition is performed by Random Forest Classifier after fusion of shape analysis-based feature and fractal-based one. In summary, the main contributions of this paper are:

– Principal line extraction from palmprint and shape analysis of resulting curves: intrinsic mean principal curve calculation, geodesic distance calculation.

– A fractal based analysis of the texture image of the palmprint.

– Fusion of fractal-based feature vector and shape analysis-based one and efficient palmprint classification.

– An extensive experimental analysis involving three different datasets which are PolyU-Palmprint dataset, CASIA-Palmprint dataset and IIT-Delhi-Palmprint-V1 dataset.

The remainder of this paper is organized as follows. The fractal analysis of the texture and the shape analysis of the principal lines are detailed respectively in Sections 3 and 4. The fusion of the texture and principal lines is presented in Section 5. The experimental settings, the dataset used and also the report results in terms of accuracy of palmprint recognition in comparison with state of the art solutions are described in Section 6. Finally, in Section 7 the concluding remarks are drawn and future research directions discussed.
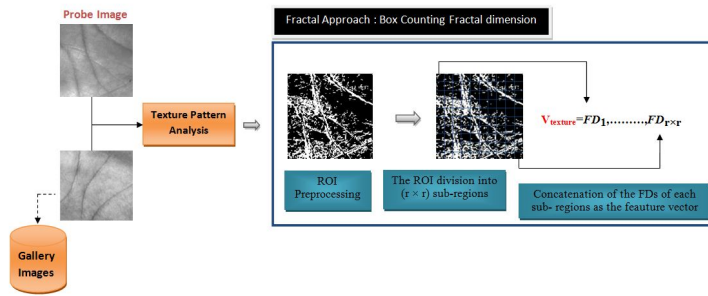
(a)

(b)
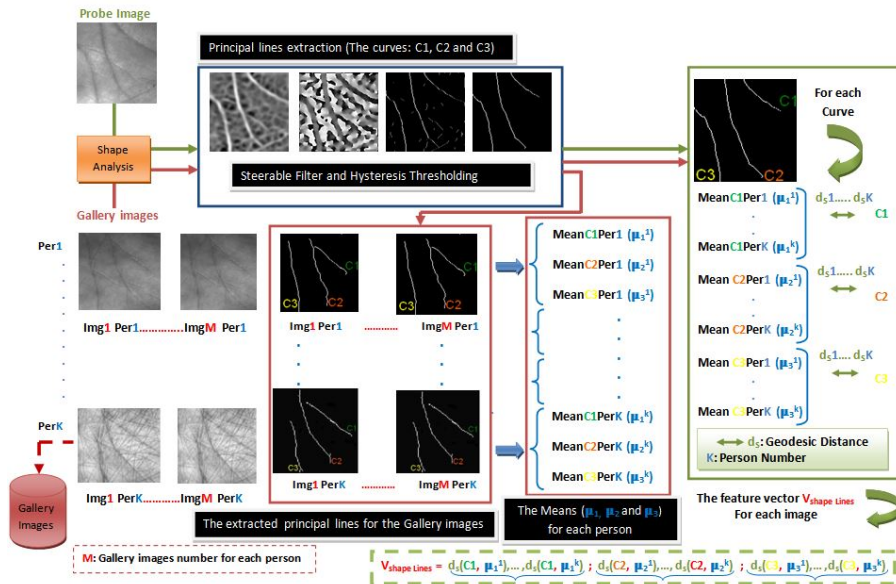
Fig. 1: Overview of the proposed method (a) The different steps of Shape analysis: in the left, the extracted principal lines for each person in the gallery data; in the middle, the calculated Means (μ_1, μ_2 and μ_3) for each person; in the right, the recognition of the given image based on the Geodesic distance (d_S) between the given curve and the obtained Means (b) The different steps of Fractal analysis: ROI Preprocessing (Binarization and edge detection of ROI), the ROI division into ($r \times r$) sub-regions and the fractal dimension for each sub-region is calculated by the box counting method.

3 Texture Analysis: Fractal

3.1 Background on Fractal Analysis

The fractal theory is an efficient technique which was developed by Mandelbrot [14] to design the objects which have a very irregular, interrupted or fragmented (geometrically complicated) shape. A fractal object is a mathematical object which comes from an iterative process and has a self-similarity character, i.e. its shape is repeated at different scales. Each object is then characterized by the Fractal Dimension that is often denoted by FD which was obtained by several methods. As will be shown in the following equation, the division of dimension D of the fractal object by a scale factor $(1/\epsilon)$ gives a number of objects: N.

$$N = (1/\epsilon)^D \tag{1}$$

The following equation represents the application of the logarithm function:

$$log(N) = D\log(1/\epsilon) \tag{2}$$

Thus, Fractal Dimension FD is determined by the following equation:

$$FD = \lim_{\epsilon \to 0} \frac{log(N(\epsilon))}{log(1/\epsilon)} \tag{3}$$

Where, $N(\epsilon)$ is the number of specimen of the initial object, $(1/\epsilon)$ is the scale factor and FD is obtained by a least squares regression method.
Nowadays, the concepts resulting from this fractal theory are used in various scientific fields like computer science, medicine and specifically in the analysis of the image texture pattern. Therefore, the texture analysis by fractal geometry is the major field in the image retrieval process. It is obtained by calculating the fractal dimension. Several methods are granted to estimate this fractal dimension of a texture pattern such as the Box Counting Method (BC), the Differential Box Counting Method (DBC), the Box Counting Density (BCD), etc. The Box Counting (BC) method is widely used for estimating the FD thanks to its effectiveness to measure the complexity and irregularity of the image texture pattern. This method is basically interested in partitioning the image space into a number of boxes (fixed-grid of square boxes) for different scales ϵ and in calculating the number of the boxes containing the information $N(\epsilon)$ for each scale.

3.2 Texture Feature vector extraction

The features extraction is a substantial step of the palmprint biometric recognition. In this paper, we investigate the applicability of the fractal dimension to extract the pertinent texture features of the palmprint. Firstly, we apply a low pass filter for reducing the noise of the ROI. Then, we extract the ROI edge
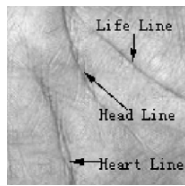
Fig. 2: The three principal lines of the palmprint

and convert each one from a grayscale image to a binary image. Afterward, we split the preprocessing ROI palmprint, successively, into $r \times r$ sub-regions equivalent square: $S_{reg}1$, $S_{reg}2$,..., $S_{reg}(r \times r)$. Therefore, we have obtained $r \times r$ sub-regions for each ROI, each of them has a normalized side S/r, where S is the size of palmprint ROI. Secondly, we calculated the fractal dimension for each sub-region (Equation 5) using the Box Counting method (BC) to describe the texture features of the palmprint. This BC method focuses on dividing each sub-region into a number of boxes for various scales ϵ and computing the number of the boxes containing the texture information $N(\epsilon)$ for each scale. The Fractal Dimension FD is obtained by a least squares regression method or the slope of the linear regression line (curve) that we plot its Y-axis which consists of the value of $log(N(\epsilon))$ against its X-axis which consists of the $log(1/\epsilon)$.

$$FD = slop\frac{log(N(\epsilon))}{log(1/\epsilon)} \qquad (4)$$

Finally, the concatenation of these fractal dimensions will be stored in a vector $\mathbf{V_{texture}}$ that represents our texture features vector for an palmprint ROI image, as described in the following equation:

$$\mathbf{V_{texture}} = FD_1, FD_2, ..., FD_{(r \times r)} \qquad (5)$$

4 Shape analysis of principal lines

4.1 Lines extraction

The principal lines convey several information which can uniquely identify an individual. There are usually three principal lines that are more noticeable, remarkable and vary somewhat over time such as life line, head line and heat line (see Fig.2). These principal lines have different orientation, depth and shape. Therefore, they are irregular even for the same palm of a person, which implies the variability intra-class and thus the difficulty of their extraction.
In this section of the paper, we present a new method to extract the principal lines of the palmprint based on the feature detection that contained two efficient descriptors like the Steerable Filter and Hysteresis Thresholding which

are suggested by the elegant work of Freeman and Adelson [15].

Steerable Filter: This filter of steerablity is a descriptor robust to noise and illumination changes. It is successfully widely-applied in a great deal of image processing and pattern recognition areas such as the image denoising [33], color image segmentation [5], texture analysis [9] and the edge detection and ridge detection [16,22], etc. In this paper, we propose steering the ridge filter to compute the ridge orientations i.e. filter with response in orientation. Thus, we follow a generic approach for ridge detector design from a class of the different functions of Steerable filter which are already observed by Jacob and Unser [20][1]. We use the second order detector of feature template which can be implemented as an Eigen-decomposition of the Hessian matrix [20] that can be interpreted in terms of Steerable filters for ridge detection [15].
Generally, the steerable filter plugin contains several parameters which are indicated as follows:
Input - The original palmprint ROI image.
M or Order - The order of the feature template Order up to 5 are supported in the current implementation i.e. $M = (1, 2, 3, 4, 5)$. Where, for edge detection M= 1, 3 or 5 and for ridge detection M= 2 or 4.
sigma (σ)- The standard deviation of the Gaussian on which the steerable templates are based. This controls the feature width.
set- Set number in case there are multiple configurations for order M.
mu (μ) - Smoothness parameters used during the filter optimization.
Filter Weights - Weight vector: Gxx, Gyy, Gxy, etc. The array of weights that control the linear combination of Gaussian derivatives up to order M which constitute the feature template.
In our experiment, the different parameters used in this paper are $M = 2$, set1 with ($\mu = 0.0$), $\sigma = 3.0$ and filter Weights Gxx=3.0 and Gyy=1.0 (The second derivation of Gaussian), as illustrated in Fig.3.
The obtained results mentioned in Figs.4.b, 4.c and 4.d correspond to the output of the ridge detection (principal lines and some strong wrinkles) based on the Steerable filter descriptor. The Steerable filter is able to extract the ridges which are contain the three principal lines and some strong wrinkles in some images. These strong wrinkles exist in some images owing to their variability inter-class and intra-class proved according to change of illumination. Next, we are interested in extracting only the principal line and thus eliminating these strong wrinkles which present the small lines.

Hysteresis Thresholding: Since the variation of illumination during the collection of the palmprint image in the dataset, the resulting extracted Ridges in some images include both principal and some strong wrinkles lines. To resolve this problem, we improve the detected ridges using Non-maximum suppression and the Hysteresis filter Thresholding which are able to reduce the probability of false ridges and fragmented lines through the following stages.

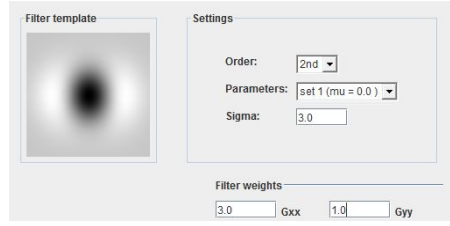[1] A Java plug-in is available at http://bigwww.epfl.ch.

Fig. 3: The different parameters of Steerable filter: The order of the feature template, The smoothness parameters used during the filter optimization, The standard deviation of the Gaussian on which the steerable templates are based and the Weights vector.
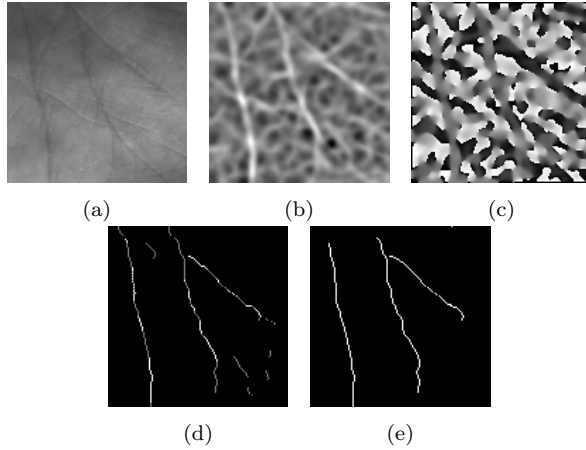

Fig. 4: Steerable Filter, Non-maximum suppression and Hysteresis Thresholding (a) The original palmprint ROI (b) The 2nd Order Response Image or the Gradient Norm Image (c) Gradient Orientation Image (d) The Ridges Detection by Non-maximum suppression and gradient parameters: $Image_{Ridge}$ (e) The final extracted principal lines: $Image_{P-Lines}$ (The Hysteresis Thresholding).

1. The input image: original palmprint ROI image (See Fig.4.a);
2. Select the obtained 2nd order response image or Gradient image (Fig.4.b);
3. Select the obtained Gradient Orientation image (Fig.4.c);
4. Apply the Non-maximum suppression to locate the lines of ridges: create new image local maxima where only local maxima should be marked as line and this image takes the same size of the original ROI palmprint image (Fig.4.d).
5. Apply the Hysteresis filter for thresholding to eliminate spurious responses. It can be seen from Fig.4.d that the resulting extracted image, $Image_{Ridge}$, includes three principal lines and some strong wrinkles. Therefore, it is necessary to determine the potential ridges and to choose two thresholds which

are T_{High} and T_{low}. Consequently, we obtained the final image (see Fig.4.e) which is called $Image_{P-Lines}$. The pseudo-code of Hysteresis Thresholding algorithm is summarized in algorithm 1.

Algorithm 1 Hysteresis Thresholding

Input: $Image_{Ridge}$: the image of ridge detection
T_{High} and T_{low}:The two thresholds
Output:$Image_{P-Lines}(x,y)$: the final principal lines image
Begin
If $Image_{Ridge}(x,y) > T_{High}$ **Then** A pixel (x,y) is called strong;
Else if $Image_{Ridge}(x,y) <= T_{low}$ **Then** A pixel (x,y) is called weak;
Else All other pixels are called candidate pixels: $Image_{P-Lines}(x,y)$
End If
  1- In each position of (x,y):
  If pixel (x,y) is weak **Then** Discard this pixel
  End If
  If pixel (x,y) is strong **Then** Take the pixel as output.
  End If
  2- If the pixel (x,y) is a candidate **Then** Follow the chain of connected local maxima in both directions along the line, as long as $Image_{Ridge}(x,y) > T_{low}$.
  End If
  3- If the starting candidate pixel (x,y) is connected to a strong pixel **Then** Take this candidate pixel as output.
  Else Not take the candidate pixel as output.
  End If
End

---

6. The final principal lines are determined using Hysteresis Thresholding based on suppressing all the ridges that are strong wrinkles and the small unconnected lines.

4.2 Background on the shapes of curves

Let $\beta : I \to \mathbb{R}^2$, represent a parameterized curve representing a principal line, where $I = [0,1]$. To analyze the shape of β, we shall represent it mathematically using the *square-root velocity function* (SRVF) [34], denoted by $q(t)$, according to: $q(t) = \frac{\dot{\beta}(t)}{\sqrt{\|\dot{\beta}(t)\|}}$; $q(t)$ is a special function of β that simplifies computations under elastic metric.

Actually, under $\mathbb{L}^2$-metric, the re-parametrization group acts by isometries on the manifold of q functions, which is not the case for the original curve β. To elaborate on the last point, let q be the SRVF of a curve β. Then, the SRVF of a re-parameterized curve $\beta \circ \gamma$ is given by $\sqrt{\dot{\gamma}}(q \circ \gamma)$. Here $\gamma : I \to I$ is a re-parameterization function and let Γ be the set of all such functions.

Define the preshape space of such curves:
$\mathcal{C} = \{q : I \to \mathbb{R}^2 | \|q\| = 1\} \subset \mathbb{L}^2(I, \mathbb{R}^2)$, where $\|\cdot\|$ implies the $\mathbb{L}^2$ norm. With the $\mathbb{L}^2$ metric on its tangent spaces, $\mathcal{C}$ becomes a Riemannian manifold. Also, since the elements of $\mathcal{C}$ have a unit $\mathbb{L}^2$ norm, $\mathcal{C}$ is a hypersphere in the Hilbert

space $\mathbb{L}^2(I, \mathbb{R}^2)$. The geodesic path between any two points $q_1, q_2 \in \mathcal{C}$ is given by the great circle, $\psi : [0, 1] \to \mathcal{C}$, where

$$\psi(\tau) = \frac{1}{\sin(\theta)} \left(\sin((1 - \tau)\theta)q_1 + \sin(\theta\tau)q_2 \right), \tag{6}$$

and the geodesic length is $\theta = d_c(q_1, q_2) = \cos^{-1}(\langle q_1, q_2 \rangle)$.

In order to study *shapes* of curves, one identifies all rotations and re-parameterizations of a curve as an equivalence class. Define the equivalent class of q as: $[q] = \text{closure}\{\sqrt{\dot{\gamma}(t)}O.q(\gamma(t)), \ \gamma \in \Gamma\}$, where $O \in SO(2)$ is a rotation matrix in $\mathbb{R}^2$. The set of such equivalence classes, denoted by $\mathcal{S} \doteq \{[q] | q \in \mathcal{C}\}$ is called the *shape space* of open curves in $\mathbb{R}^2$. As described in [34], $\mathcal{S}$ inherits a Riemannian metric from the larger space $\mathcal{C}$ due to the quotient structure. To obtain geodesics and geodesic distances between elements of $\mathcal{S}$, one needs to solve the optimization problem:

$$(O^*, \gamma^*) = argmin_{\gamma \in \Gamma, O \in SO(2)} d_c(q_1, \sqrt{\dot{\gamma}}O.(q_2 \circ \gamma)). \tag{7}$$

The optimization over Γ is done using the dynamic programming algorithm for a fixed O in $SO(2)$, and the optimization over $SO(2)$ is performed using SVD for a fixed $\gamma \in \Gamma$. The solution is reached by iterating over the two previous steps. Let $q_2^*(t) = \sqrt{\dot{\gamma^*}(t)}O^*.q_2(\gamma^*(t)))$ be the optimal element of $[q_2]$, associated with the optimal re-parameterization γ^* of the second curve and the optimal rotation O^*, then the geodesic distance between $[q_1]$ and $[q_2]$ in $\mathcal{S}$ is $d_s([q_1], [q_2]) \doteq d_c(q_1, q_2^*)$ and the geodesic is given by Eqn. 6, with q_2 replaced by q_2^*. This representation was previously investigated for biometric [10,12,1,11] and soft-biometric applications [39,2] based on the face shape.

4.3 Mean calculation of principal lines

One advantage of a shape analysis framework of the principal lines is that one has the actual deformations in addition to distances. In particular, we have a geodesic path in $\mathcal{S}$ between the two curves β^1 and β^2 in $\mathbb{R}^2$. This geodesic corresponds to the optimal elastic deformations of two curves. We can use our framework to calculate some statistics as the "mean" of curves in the space of the shape of the curves lying in $\mathbb{R}^2$.

The Riemannian structure defined on the manifold of shape of the curves in $\mathcal{S}$ enables us to perform such statistical analysis for computing principal lines means and variance. The Karcher mean utilizes the intrinsic geometry of the manifold to define and compute a mean on that manifold. It is defined as follows: let $d_s(\beta^i, \beta^j)$ denote the length of the geodesic from β^i to β^j in $\mathcal{S}$. To calculate the Karcher mean of curves $\{\beta^1, ..., \beta^n\}$ in $\mathcal{S}$, define the variance function:

$$\mathcal{V} : \mathcal{S} \to \mathbb{R}, \mathcal{V}(\beta) = \sum_{i=1}^{n} d_s(\beta, \beta^i)^2 \tag{8}$$

The Karcher mean is then defined by:

$$\mu = \arg\min_{\eta \in \mathcal{S}} \mathcal{V}(\eta) \tag{9}$$

The intrinsic mean may not be unique, i.e. there may be a set of points in $\mathcal{S}$ for which the minimizer of $\mathcal{V}$ is obtained. To interpret geometrically, $\overline{\beta}$ is an element of $\mathcal{S}$, that has the smallest total deformation from all given curves. We present a commonly used algorithm for finding Karcher mean for a given set of line curves. This approach, presented in algorithm 2, uses the gradient of $\mathcal{V}$, in the space $T_\mu(\mathcal{S})$, to iteratively update the current mean μ.

Algorithm 2 Karcher mean algorithm

Set k = 0. Choose some time increment $\epsilon \le \frac{1}{n}$. Choose a point $\mu_0 \in \mathcal{S}$ as an initial guess of the mean. (For example, one could just take $\mu_0 = \beta^1$.)

1- For each $i = 1, ..., n$ choose the tangent vector $t_i \in T_{\mu_k}(\mathcal{S})$ which is tangent to the geodesic from μ_k to β^i. The vector $g = \sum_{i=1}^{i=n} t_i$ is proportional to the gradient at μ_k of the function $\mathcal{V}$.

2- Flow for time ϵ along the geodesic which starts at μ_k and has velocity vector g. Call the point where you end up μ_{k+1}.

3- Set $k = k + 1$ and go to step 1.

Since this is a gradient approach, it only ensures a local minimizer of the variance function $\mathcal{V}$.

The motivation for using statistical means of shapes in a biometric application is to represent several principal lines belonging to the same class by an intrinsic mean shape. The feature vector for a curve classification is based on the calculated means.

4.4 Shape Feature vector

The feature vector is built using the distances to the means of the principal line curves belonging to the same persons, calculated on train data as follow. Given train sets $T_1 = \{\beta_1^1, ..., \beta_1^n\} \in \mathbb{R}^{2 \times n}$, $T_2 = \{\beta_2^1, ..., \beta_2^n\} \in \mathbb{R}^{2 \times n}$, and $T_3 = \{\beta_3^1, ..., \beta_3^n\} \in \mathbb{R}^{2 \times n}$ holding respectively C_1, C_2 and C_3 curves, belonging to k different persons. Where n is the curve number of same type C_i in the train data. Each curve corresponds to a person $label_j \in \{Per_1, ..., Per_k\}$. We first calculate, using algorithm 2, the means μ_1^j, μ_2^j and μ_3^j for each class (person). Next, we calculate the geodesic distance d_S between a given curve β and the mean curves of the same type (C_1, C_2 or C_3). Thus a vector of distance of size k is provided as feature vector to classify the curve β.

In order to classify the principal lines provided by a palmprint, we concatenate the feature vectors for the corresponding β_1, β_2 and β_3 of types C_1, C_2 and C_3 respectively. the palmprint resulting feature vector, denoted $\mathbf{V_{shape\ Lines}}$, includes the distances between β_1 and the curves of type C_1, β_2 and the curves

of type C_2 and β_3 and the curves of type C_3; the size of the feature vector is $k \times 3$.

$$\mathbf{V_{shape\ Lines}} = (d_S(C_1, \mu_1^1), d_S(C_1, \mu_1^2), ..., d_S(C_1, \mu_1^k)),$$
$$(d_S(C_2, \mu_2^1), d_S(C_2, \mu_2^2)..., d_S(C_2, \mu_2^k)), \qquad (10)$$
$$(d_S(C_3, \mu_3^1), d_S(C_3, \mu_3^2)..., d_S(C_3, \mu_3^k))).$$

5 Fusion of shape and texture for palmprints recognition

5.1 Feature vector building

Feature fusion is a good way to improve the performance and increase the system accuracy. In this paper, the features are issued from the same modality: thus they are called intra-modal features.

Several levels of fusion have been presented in literature to reach the robustness of system such as, (1) fusion at feature level, (2) fusion at feature score level and (3) fusion at feature decision level. In this paper, we focus on the feature level fusion that concatenates the features vectors: $\mathbf{V_{texture}}$ and $\mathbf{V_{shape\ Lines}}$ of a palmprint which are obtained using Fractal as well as Shape Analysis, respectively.

5.2 Classification

For the classification phase, we used the Multi-class version of Random Forest algorithm. This algorithm was proposed by Leo Breiman in [3] and defined as a meta-learner comprised of many individual trees. It was designed to quickly operate over large datasets and more importantly to be diverse by using random samples to build each tree in the forest. Diversity is obtained by randomly choosing attributes at each node of the tree and then using the attribute that provides the highest level of learning. Once trained, Random Forest classifies a new person from an input feature vector by putting it down each of the trees in the forest. Each tree gives a classification decision by voting for this class. Then, the forest chooses the classification having the most votes (over all the trees in the forest). In our experiments, we used Weka Multi-class implementation of Random Forest algorithm by considering 250 trees. A study of effect of the Tree number is mentioned later in the experimental result part.

6 Experimental results

This section recapitulates our empirical results and provides an analysis of the performance of our method compared to other state-of-the-art results

using three large datasets which are "PolyU-Palmprint" dataset, "CASIA-Palmprint" dataset and "IIT-Delhi-Palmprint" dataset. The main results of these datasets are reported in the following sub sections.

6.1 Data Pre-processing

The palmprint data pre-processing step is a prerequisite and nontrivial in the biometric system. It consists in extracting the region of interest (ROI) of the palmprint using several operations [30], [29]. As illustrated in Fig.5, this data preprocessing step includes the following items:

– *Binarization:* The grayscale original image is first converted into binary image by using the Otsu's method [31], based on the segmentation of the input image into foreground and background.
– *Morphology Operations:* Sometimes, the users put their hands with rings, which can create a problem of identification. In order to solve and avoid this problem, the morphology operations: the closing and the opening operations, are used.
– *Edge Detection:* the edge of the image is detected and a smoothing filter (low pass filter) is applied to eliminate the noise and remove the holes curve.
– *Coordinate System Stabilization:* the key points between the fingers (specifically the two finger-webs: $Pw1$ and $Pw2$ as indicated in Fig.5) are extracted in order to stabilize the coordinate system which is able to successfully locate the region of interest ($F1F2F3F4$) in the form of a square. Then, a mask having the same coordinate of this resulting square on the original image is applied to correctly extract the ROI from the rest of the hand.
– *ROI Normalization:* this step consists of the following phases:
  Firstly, the palmprint images must be resized to a standard dimension since they may have different sizes due to variability from one hand to another. Hence, they must fix the size of the located ROI to $T \times T$ with T=150 pixels. Secondly, the extracted ROI should be rotated to a vertical position as the palmprint images were taken with different orientations. Finally, a low pass filter is applied to reduce the noise in order to improve the quality of the extracted ROI.

6.2 Comparative evaluation on the PolyU-Palmprint dataset

The Hong Kong Polytechnic University PolyU-Palmprint dataset was acquired by collecting 8000 palmprint images captured from 400 different subjects. Each subject is represented by twenty samples acquired in two sessions (10 samples by session). The average time interval between the two sessions is one month. The capture system captures the palmprint images using a real time CCD
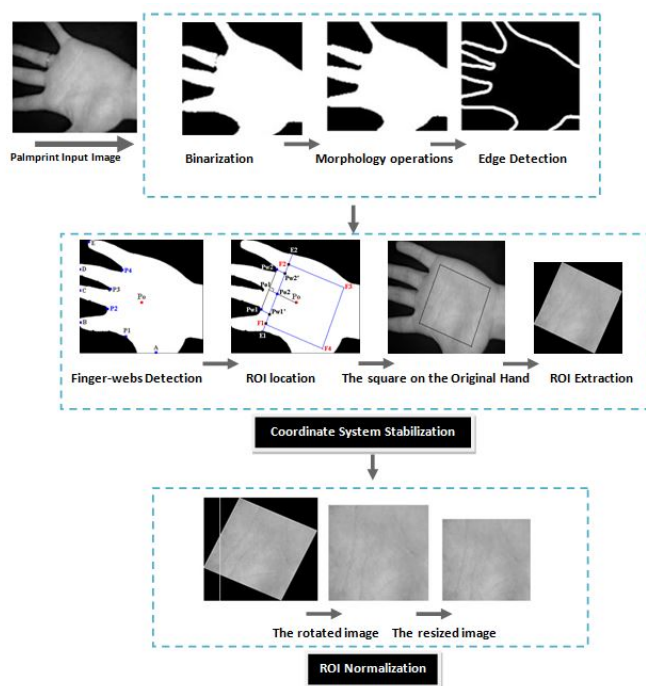
Fig. 5: Flow chart of the palmprint preprocessing step: There are various pipelines for this step. Namely, the pipelines are (1) Binarization, (2) Morphology Operations: the closing and the opening operations, (3) Edge Detection, (4) Coordinate System Stabilization and ROI extraction, and (5) ROI Normalization: The resizing and rotating of ROI.

capture device. All palmprint images of this dataset are 8 bits graylevel, BMP format and the size of each of them is 384×284 pixels. These images collected in the same position and direction in the two sessions which implies that all users have the freedom to hold their hands on the capture system with any restriction. In addition, segmented region of interest (ROI) which represents palmprint images are also available in this database. The size of each 2D ROI is 128×128 pixels. Furthermore, there is a variation and a change of the distributed illumination between the first and the second sessions which brings the difficulty of the person's identification.

Fig.6 shows the used capture system, some examples of these palmprint images.

Fig.7 depicts four palmprint ROI images of PolyU database, which were captured from a same person but in different sessions. This figure presents the first two images which were captured in the 1st session and the last two images which were captured in the second session. It can be noticed that there are great changes of illumination between these images captured in different

sessions.

We assess the performance of our approach for palmprint identification based
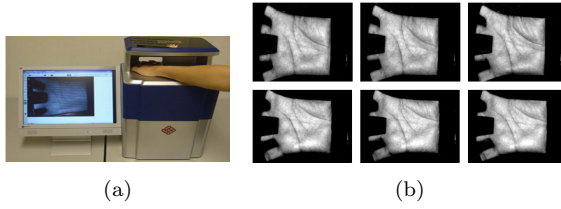

Fig. 6: Palmprint Image Scan of "PolyU-Palmprint" dataset (a) The used capture system (b) Some examples of the palmprints.
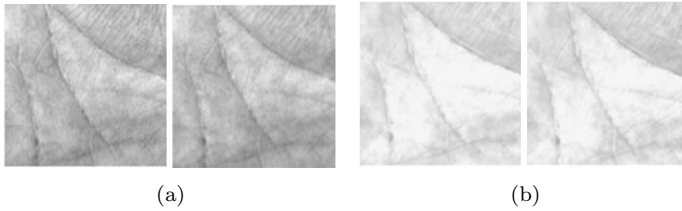

Fig. 7: Four palmprint ROI images from a same person in PolyU database (a) two images captured in the first session (b) two images captured in the second session.

on two experiments with this dataset.

In the first experiment, we randomly selected 7 samples of each person which were taken from the 1st session as the gallery data and the remaining samples of the same session (1st session) make up the probe data. Therefore, we used 2800 samples for gallery data (Train) and 1200 samples for probe data (Test).

In the second experiment, all the 10 samples of each person which were taken from the 1st session built the gallery data and 5 randomly selected samples from the 2st session make up the probe data. Therefore, we used 4000 samples for gallery data (Train) and 2000 samples for probe data (Test).

In order to make a fair performance comparison, we presented two types of comparisons between the proposed approach and the most famous systems in the state-of-the-arts using similar protocols. The difference between the presented protocols lies in the number of users considered in both the gallery and the probe data. We present the results on this dataset in three different tables: Table 1 compares our principal line results with the principal lines based on the state-of-art methods. In Table 2, we present a comparative study of texture-based results of the proposed approach with the state-of-the art

Table 1: Recognition results of the extracted principal lines comparison of the state-of-the-art results on the PolyU-Palmprint database. Protocols Description: Samples of person (S), Users in dataset (U), Gallery data (G), Probe Data (P).

Approaches	Descriptors	Protocols	RRs-with Experiment1	RRs-with Experiment2
khan et al. [24]	Delaunay-Triangulation	50 U, 6 S, –, –	90.00%	–
Hu et al.[19]	Modified-Finite-Radon-Transform (MFRAT)	100 U, 6 S, 3 G, 3 P	92.50%	–
Krichneswari et al.[25]	wavelet transform	100 U, 15 S, 5 G, 10 P	–	73.65%
Tunkpienne et al.[36]	Consecutive-Gradient+ Morphological operators	–, –, –, –	86.18%	–
Our approach	Steerable Filter and Karcher Mean	400 U, 10 S, 7 G, 3 P	93.13%	–
		400 U, 15 S, 10 G, 5 P	–	91.00%
		400 U, 15 S, 5 G, 10 P	–	88.89%

of texture based approaches. Table 3 presents the results of the proposed approach in comparison with the intra-modal state-of-the art methods.

As illustrated in Table 1, for the first experiment, although the number of users used for testing is bigger in our first experiment compared to well-known methods, where only 100 users are considered, the proposed approach outperforms the totality of previous approaches. Obviously, this performance of Recognition Rate (RR) reaches 93,13%, which brings the improvement rates of about 3.13 %, 0.63 % and 6.95%, respectively to the result in [24], [19] and [36]. On the other hand, in the second experiment, we observed yet a better RR than the work in [25]. This performance of RR reaches 91,00% when we use the 10 samples for the gallery data and 5 samples for the probe data in the matching phase. This scenario is important in a real application where gallery and probe data are acquired in different sessions. To make the fair comparison with that krishneswari et al.[25], we further test the proposed approach using the same setting of Samples classification for gallery data and probe data proposed by the work described in krishneswari et al.[25] (5 samples in the gallery data and 10 samples for the probe data). It can be concluded from this result that the proposed approach likewise yields a better performance of Recognition Rate compared to the other work but it cannot gives a better recognition rate than the first sample classification. Hence, it is necessary to increase the number of samples (images) in the gallery data. This is in concordance with the results provided by Hammami et al. [17] and Tana et

Table 2: Recognition results of the extracted texture comparison of the state-of-the-art results on the PolyU-Palmprint database. Protocols Description: Samples of person (S), Users in dataset (U), All Users, Gallery data (G), Probe Data (P).

Approaches	Descriptors	Protocols	RRs-with Experiment1	RRs-with Experiment2
Hu et al.[19]	Gabor Filters	100 U, 6S, 3G,3P	84.30%	–
	DWT	All users, –, –	95.20%	–
Khalifa et al.[23]	CM	All Users, –, –	91.19%	–
	Gabor Filters	All Users, –, –	90.57%	–
Hammami et al. [17]	LBP+ SFFS	All Users,10 G,10 P	–	95.35%
Krichneswari et al. [25]	Gabor filters	100U, 15S, 5G, 10S	–	83.35%
Wang et al.[37]	2D-Gabor-Wavelet +PCNN	All Users, 5G, 5P	97.37%	–
		All Users, 5G, 10P	–	95.48%
		All users, 7 G, 3 P	96.65%	–
Our approach	Fractal (FDBC)	All users, 10 G, 5 P	–	95.31%
		All users,5 G, 10 P	–	95.00%

Table 3: Recognition results of the extracted Intra-modal features comparison of the state-of-the-art results on the PolyU-Palmprint database. Protocols Description: Samples of person (S), Users in dataset (U), All Users, Gallery data (G), Probe Data (P).

Approaches	feature fusion	Protocols	RRs-with Experiment1	RRs-with Experiment2
Hu et al.[19]	Principal lines +Eigen-Palm+Texture	100 U, 6 S, 3 G,3 P	98.00%	–
Krichneswari et al.[25]	Texture+ Line+Appearance	100 U, 15 S, 5 G, 10 P	–	94.89%
Zhi et al.[40]	Texture+ Principal lines	all users, 1 G, 9 P	97.82%	–
Our approach	Texture Pattern +Principal lines shape	all users, 7 G, 3 P	**98.32**%	–
		all users, 10 G, 5 P	–	96.99%
		all users, 5 G, 10 P	–	96.45%

al. [35], where they show that it is important that the sample number in the training data (gallery data) be high to achieve a best performance of RR.

Table.2 summarizes approaches and results of texture Analysis reported previously on the PolyU dataset, compared to those obtained in this work. The testing protocols used in the experiments are quite different, especially the number of samples in the gallery data and probe data, except in [23] where the number of sets of gallery and probe is not specified. The number of users considered represent all the users of the dataset (400 users) in several works, except in [19] and [25] where the number of users is restricted to 100.

In [37], the results are presented for palmprint recognition accuracy on all subjects picked out from the PolyU dataset. The authors improve the performance with two experiments. In the first experiment, 5 samples of each subject from the 1st session are selected for the gallery data and 5 samples of the same session for the probe data. In the second experiment, 5 samples from the 1st session are selected for the gallery data and 10 samples from the 2st session are selected for the probe data. The best recognition scores on PolyU for two experiments are reported by Wang et al. [37] which are 97.37% and 95.48%, respectively. In order to keep the comparisons fair, we kept the 5 samples in the gallery and 10 samples in the probe. it should be noticed that our method achieved a 95.00% recognition which is close to the highest published result on this sample classification in the second experiment [37]. It can be concluded that the obtained results of our proposed approach give a better performance of Recognition Rates than the outcomes of the works in [23], [19] and [25]. Furthermore, according to this comparative analysis, the proposed approach is favorably comparable with the best state-of-the-art solutions [17] and [37].

Table. 3 recapitulates a comparison of the obtained results of this work with previous works in intra-modal features extraction. Compared to our work, the works in [19] and [25] focus on a small dataset user number, which leaves uncertainty about the statistical significance of their performance on large and important challenging dataset. These two works fuse three features of palmprint. Nevertheless, Zhi et al. [40] combine two features of the palmprint as our proposed approach such as the texture pattern and the principal line shape of the palmprint. Hu et al.[19] and Zhi et al. [40] provide their experiments with the classification of samples in the same session for the gallery data and the probe data. The work of [25] that uses the mixture between two sessions of the dataset for samples classification as ours yielded 94.89% recognition rate, whereas we reached a 96.99% for 10 and 5 samples in the gallery data and probe data, respectively and 96.45% during the use of the same sample classification in [25].

The most similar work to ours is provided in [40]. With all the subjects of PolyU and principal lines and texture fusion, [40] achieved 97.82% recognition rate, while we achieved a much higher result of 98.32% by combining Principal Line Shape and Texture Pattern. From this table, it can be seen that the proposed feature fusion approach achieves the best performance.

Since scans in PolyU have high quality, many methods are able to provide good performance and especially when using the images from the same session. It is, thus, important to evaluate a method in other situations where the data quality is not as good. In the next two sections, we will consider those situations

with the CASIA and the IITDelhi datasets involving the scale variations, the direction and posture challenges.

6.3 Comparative evaluation on the CASIA-Palmprint dataset

The CASIA-Palmprint dataset contains 5502 palmprint images captured from 312 subjects. This dataset is taken from Chinese Academy of Sciences of institution who Automation. All palmprint images of this dataset are 8 bits graylevel and JPEG format. For each subject, 8 palmprint images have been collected from both left and right palms. The resolution of original palmprint images is 640×480 pixels. The capture system captures the all palmprint images using a CMOS camera fixed on the top of the device. This latter supplies an evenly distributed illumination on the palmprint images. Since the hand of each person is not touching any platform plate, a presence of distance variation between the hand and the capture device which implies scale variations. In this dataset, the users are not used the guidance pegs to constraint their hands (unconstrained peg-free setup). Therefore, these hand images are captured with different directions and postures, which brings on contracting and stretching the principal lines and texture skin pattern at the region of interest of the palmprint. This dataset has many variations which make the identification of the persons more difficult. Fig.8 shows the capture system used and some examples of these palmprint images in the database.
This database was automatically preprocessed as described in the Section 6.1.
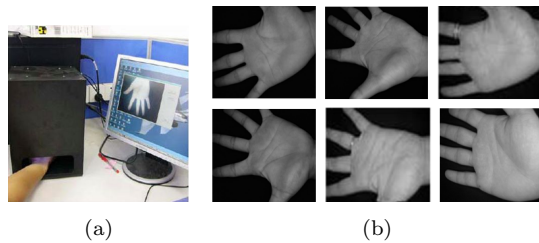

(a)   (b)

Fig. 8: Palmprint Image Scan of "CASIA-Palmprint" dataset (a) the capture system (b) Some examples of the palmprints.

Since the CASIA dataset contains numerous challenging and variation in term of scales, position, direction, etc, the principal lines and Intra modal approaches with this dataset are currently almost absent in literature. Except, Bruno et al. [4] proposed an approach to detect the principal lines and thus achieved 80.00% recognition rate, while we achieved a much higher result of 92.98%, as mentioned in Table 4. Hence, we observed that the performance of the principal line extraction has a very high recognition rate compared to the work in [4].

Table 4: Recognition results comparison of the state-of-the-art results on the CASIA-Palmprint database. Protocols Description: Right hand (R), left hand (L), Samples of person (S), Gallery data (G), Probe Data (P).

Approaches	Protocols	Features extraction		
		Principal lines	Texture-Pattern	Intra-modal
Bruno et al.[4]	–, 8 S, –, –	80.00%	–	–
Jawsal et al.[21]	R, 8 S, –, –	–	90.76%	–
Hammami et al.[17]	(R and L), 8 S, 5 G, 3 P	–	97.53%	–
Our approach	(R and L) 8 S, 5 G,3 P	92.98%	96.00%	**98.00%**
	R, 8 S, (5 G,3 P)	–	96.52%	–

In order to make the comparison of our texture extraction method fair, we kept the same setting protocols using by Jawsal et al. [21] (only the right hand of the dataset). Our method outperforms their approach with a performance of 96.52%. Consequently, this result presents an improvement rate of about 5.76%.

We conducted tests of the texture extraction by following the same testing protocol proposed by the evaluation described in [17], we have achieved comparable results than in this work.

It is worth noting that there is no prior result in the literature on palmprint recognition by feature fusion (Intra-modal approaches) using this dataset, while, we have a significant recognition rate of about 98.00%, which is the best result on this dataset.

6.4 Comparative evaluation on the IIT-Delhi-Palmprint-V1 dataset

The IITD-Palmprint dataset contains 2300 palmprints images captured from 230 individuals aged from 14 to 56 years. All images of this dataset have been acquired by using a digital CMOS camera and saved in bitmap format. For each individual, 5 palmprint images are acquired in varying hand pose variations and have been collected from both left and right palms. So, 1150 left palmprints and 1150 right palmprints. All the images are collected in the indoor environment and employ circular fluorescent illumination around the camera lens. Each person is provided to present his/her hand in the imaging region with different positions and directions which deal the scale variations. In addition, the automatically cropped and segmented palmprint images (region of interest-ROI) are also available in this dataset with size 150×150 pixels.

We randomly selected 3 samples of each person for the gallery data and the remaining samples are used as probe data (2 samples). Tables 5 and 6 compare

the results of our method with the previously published results following the principal lines and texture extraction, respectively. The setting protocols of the number of users considered represent all the users of dataset (230 users) in the several experiments works, except in [26] where the number of users is restricted to 100 users.

As noted, our approach provides the highest recognition rate for palmprint with principal line shape extraction (92.82%) and texture pattern extraction (95.80%).

Table 5: Recognition results of the extracted principal lines comparison of the state-of-the-art results on the IIT-Delhi-Palmprint-V1 database. Protocols Description: Samples of person (S), Users in dataset (U), Gallery data (G), Probe Data (P).

Approaches	Descriptors	Protocols	RRs
Kumar et al.[26]	Radon transform	100 U, 5 S, −, −	92.80%
Our Approach	Steerable-Filter and Karcher-Mean	230 U, 5 S, 3 G, 2 P	92.82%

Table 6: Recognition results of the extracted texture comparison of the state-of-the-art results on the IIT-Delhi-Palmprint-V1 database. Protocols Description: Samples of person (S), Users in dataset (U), Gallery data (G), Probe Data (P).

Approaches	Descriptors	Protocols	RRs
Kumar et al.[26]	Gabor Filters	100 U, 5 S, −, −	95.00%
Charfi et al.[7]	SIFT	230 U, 6 S, 3 G, 2 P	94.05%
Jawsal et al.[21]	Gabor+PCA+LDA	230 U, 6 S, −, −	91.40%
Our Approach	Fractal (FDBC)	230 U, 5 S, 3 G, 2 P	95.80%

We observed in Table 7 that the performance of our intra-modal approach is very high with a recognition rate of about 97.98% compared to the work of Luo et al. [28] (92.00%) which follows the same protocol as ours. Consequently, this result presents an improvement rate of about 5.98%. We have achieved comparable results with Kumar et al. [26]. These researchers achieved about 0.77% higher recognition rate than us, they considered only 100 users while we achieved our results using all the subjects on database.

Table 7: Recognition results of the extracted Intra-Modal features comparison of the state-of-the-art results on the IIT-Delhi-Palmprint-V1 database. Protocols Description: Samples of person (S), Users in dataset (U), Gallery data (G), Probe Data (P).

Approaches	Descriptors	Protocols	RRs
Kumar et al.[26]	Texture(Gabor)+ EigenPalm+Principal lines	100 U,5 S, −, −	98.75%
luo et al.[28]	texture (LBP)+Principal lines (LLDP)	230 U, 5 S,1 G, 4P	92.00%
Our Approach	Texture+Principal lines	230 U, 5 S, 3 G, 2 P	97.98%

6.5 Effect of number of ROI division

In order to validate the choice of 10 as a number of the ROI division into sub-regions, we presented the following Table.8. It shows the result of recognition rates of the PolyU-Palmprint dataset achieved in our experiments which was noticed for 12 different splits of ROI into sub-region (See Fig.9). We studied

Table 8: The achieved recognition rates by applying the Fractal descriptor with different splits of ROI

RRs %	1*1	2*2	3*3	4*4	5*5	6*6	7*7	8*8	9*9	**10*10**	11*11	12*12
Texture-Pattern Fractal (FDBC)	88.50	92.50	93.60	94.35	94.50	94.00	94.80	95.50	96.00	**96.65**	96.20	95.00

the recognition rates of the PolyU-dataset achieved by applying the Fractal descriptor for the different divisions of ROI palmprint image into sub-regions and thus it can be concluded that division 10 gives the best Recognition Rate. We apply the same number of divisions for all our experiments.

6.6 Effect of the number of trees in Random Forest algorithm

The performance of Random Forest classifier changes with the different number of trees. Therefore, we perform the experiments with several number of trees; thus, the obtained results are illustrated in Table.9 and depicted in Fig.10. These experiments demonstrate that the recognition rates rise with the increasing number of trees until 250, and then become quite decrease. Thus, the best recognition rates are 96.65%, 93.13% and 98.32% for texture
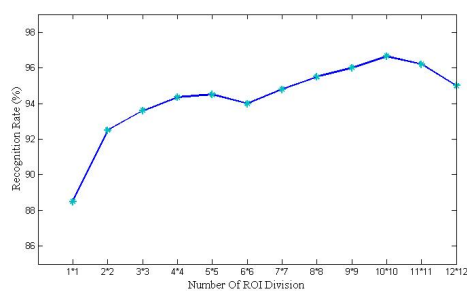
Fig. 9: Palmprint identification results using a Fractal Analysis Descriptor with different number of ROI Division.

analysis, shape analysis and intra-modal analysis, respectively; achieved by 250-Tree Random Forest.

Table 9: The different Recognition Rates with several number of trees of Random Forest.

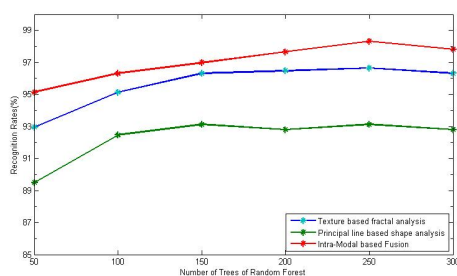| Tree Number	Fractal	Karcher Means	Fractal+Karcher Means
50	92.96%	89.94%	95.14%
100	95.14%	92.46%	96.31%
150	96.31 %	93.13%	96.98%
200	96.48 %	92.7973%	97.65%
250	**96.65**%	**93.13**%	**98.32**%
300	96.31%	92.79 %	97.82%

Fig. 10: Palmprint identification results using a Random Forest when varying the number of trees: Intra-modal approach based fusion (Red curve), Principal lines based shape analysis (green curve) and Texture analysis (blue curve)

6.7 Discussion

In order to study the performance of the proposed approach in the presence of different challenges, we have presented experimental results using three well-known palmprint datasets. The results of our proposed intra-modal approach which are achieved in these two experiments are shown in Table.10. It is clear that these results show that the first experiment reaches 98.32 % which is a superior compared to the second experiment. This is due to the protocols of the second experiment which are a mixture of images between two sessions. This is important in a real application thanks to the several changes and variability in terms of lighting conditions (illumination), which vary from one session to another. The objective of this experiment is to verify the robustness of our proposed method. This second experience recorded an identification rate of about 96.99 %. Another conclusion that can be made from Table 10 is that the fractal features achieve a better performance compared to the principal line features. The performance improvement is due to the combination of two palmprint representations can be observed in row three of Table.10.

Table 10: The different Recognition Rates of our experiments for the three datasets and the different experiments

Proposed Approaches		Datasets – (RRs%)			
Features Extraction	Descriptors	PolyU		CASIA	IIT-Delhi-Palmprint
		Experiment1	Experiment2		
Principal-lines	Steerable-Filter+ Karcher Mean	93,13 %	91.00 %	92.98 %	92.82 %
Texture-Pattern	Fractal (FDBC)	96.65 %	95.31 %	96.00 %	95.80 %
Intra-Modal	features-fusion level	98.32%	96.99 %	98,00 %	97.98 %

7 Conclusion

In this paper, we have presented a framework for intra-modal palmprint recognition. The texture and the principal lines are investigated separately. An elastic shape analysis framework is used in order to analyze the shape of the principal lines. This framework has the advantage to provide re-parameterization invariant distance between the principal lines and also to compute some statistics like the intrinsic means which are to make the feature vectors for principal line classification. The texture information is also investigated using the fractal analysis. The fusion of the resulting features makes an efficient method for palmprint recognition with different challenges. This is validated by comparative studies on three challenging datasets; the proposed approach performs

competitive results using the principal lines, the texture and the intra-modal fusion. As future work, we plan to integrate in our approach the feature selection techniques which can be used to reduce the dimensionality of the features and thus increase the recognition accuracy.

References

1. Amor, B.B., Drira, H., Ballihi, L., Srivastava, A., Daoudi, M.: An experimental illustration of 3d facial shape analysis under facial expressions. Annales des Télécommunications 64(5-6), 369–379 (2009)
2. Amor, B.B., Drira, H., Berretti, S., Daoudi, M., Srivastava, A.: 4-d facial expression recognition by learning geometric deformations. IEEE Trans. Cybernetics 44(12), 2443–2457 (2014)
3. Breiman, L.: Random forests. Machine learning 45(1), 5–32 (2001)
4. Bruno, A., Carminetti, P., Gentile, V., La Cascia, M., Mancino, E.: Palmprint principal lines extraction. In: Biometric Measurements and Systems for Security and Medical Applications (BIOMS) Proceedings, 2014 IEEE Workshop on. pp. 50–56. IEEE (2014)
5. Burlacu, C., Burlacu, G.: Color image segmentation using steerable filters. In: Signals, Circuits and Systems, 2005. ISSCS 2005. International Symposium on. vol. 1, pp. 347–350. IEEE (2005)
6. Chaabouni, A., Boubaker, H., Kherallah, M., Alimi, A.M., El Abed, H.: Fractal and multi-fractal for arabic offline writer identification. In: Pattern Recognition (ICPR), 2010 20th International Conference on. pp. 3793–3796. IEEE (2010)
7. Charfi, N., Trichili, H., Alimi, A.M., Solaiman, B.: Bimodal biometric system based on sift descriptors of hand images. In: Systems, Man and Cybernetics (SMC), 2014 IEEE International Conference on. pp. 4141–4145. IEEE (2014)
8. Chen, J., Zhang, C., Rong, G.: Palmprint recognition using crease. In: Image Processing, 2001. Proceedings. 2001 International Conference on. vol. 3, pp. 234–237. IEEE (2001)
9. Do, M.N., Vetterli, M.: Rotation invariant texture characterization and retrieval using steerable wavelet-domain hidden markov models. Multimedia, IEEE Transactions on 4(4), 517–527 (2002)
10. Drira, H., Amor, B.B., Daoudi, M., Srivastava, A.: Pose and expression-invariant 3d face recognition using elastic radial curves. In: British machine vision conference. pp. 1–11 (2010)
11. Drira, H., Amor, B.B., Srivastava, A., Daoudi, M., Slama, R.: 3d face recognition under expressions, occlusions, and pose variations. IEEE Trans. Pattern Anal. Mach. Intell. 35(9), 2270–2283 (2013)
12. Drira, H., Boulbaba, B.A., Anuj, S., Mohamed, D.: A riemannian analysis of 3d nose shapes for partial human biometrics. In: International Conference on Computer Vision. pp. 2050–2057 (2009)
13. Duta, N., Jain, A.K., Mardia, K.V.: Matching of palmprints. Pattern Recognition Letters 23(4), 477–485 (2002)
14. Fractals, M.B.L.O.: Forme, hasard et dimension. Paris: Flammarion (1975)
15. Freeman, W.T., Adelson, E.H.: The design and use of steerable filters. IEEE Transactions on Pattern Analysis & Machine Intelligence (9), 891–906 (1991)
16. González Serrano, G., Fleuret, F., Aguet, F., Benmansour, F., Unser, M., Fua, P.: Rotational features extraction for ridge detection. Institute of Electrical and Electronics Engineers (2011)
17. Hammami, M., Jemaa, S.B., Ben-Abdallah, H.: Selection of discriminative sub-regions for palmprint recognition. Multimedia tools and applications 68(3), 1023–1050 (2014)
18. Han, C.C., Cheng, H.L., Lin, C.L., Fan, K.C.: Personal authentication using palm-print features. Pattern recognition 36(2), 371–381 (2003)

19. Hu, J., Xue, Y., Zhao, Y., Lu, J.: Palmprint recognition based on multiple feature information fusion. In: Signal Processing, 2008. ICSP 2008. 9th International Conference on. pp. 1449–1452. IEEE (2008)
20. Jacob, M., Unser, M.: Design of steerable filters for feature detection using canny-like criteria. Pattern Analysis and Machine Intelligence, IEEE Transactions on 26(8), 1007–1019 (2004)
21. Jaswal, G., Nath, R., Kaul, A.: Texture based palm print recognition using 2-d gabor filter and sub space approaches. In: Signal Processing, Computing and Control (ISPCC), 2015 International Conference on. pp. 344–349. IEEE (2015)
22. Jose, A., Krishnan, S.R., Seelamantula, C.S.: Ridge detection using savitzky-golay filtering and steerable second-order gaussian derivatives. In: Image Processing (ICIP), 2013 20th IEEE International Conference on. pp. 3059–3063. IEEE (2013)
23. Khalifa, A.B., Rzouga, L., BenAmara, N.E.: Wavelet, gabor filters and co-occurrence matrix for palmprint verification. International Journal of Image, Graphics and Signal Processing 5(8), 1 (2013)
24. Khan, Z.N., Qureshi, R.J., Ahmad, J.: On feature based delaunay triangulation for palmprint recognition. arXiv preprint arXiv:1602.01927 (2016)
25. Krishneswari, K., Arumugam, S.: Intramodal feature fusion based on pso for palmprint authentication. Int Journal on Image and Video Proc 2(4), 435–440 (2012)
26. Kumar, A., Shekhar, S.: Palmprint recognition using rank level fusion. In: Image Processing (ICIP), 2010 17th IEEE International Conference on. pp. 3121–3124. IEEE (2010)
27. Kumar, A., Zhang, D.: Personal authentication using multiple palmprint representation. Pattern Recognition 38(10), 1695–1704 (2005)
28. Luo, Y.T., Zhao, L.Y., Zhang, B., Jia, W., Xue, F., Lu, J.T., Zhu, Y.H., Xu, B.Q.: Local line directional pattern for palmprint recognition. Pattern Recognition 50, 26–44 (2016)
29. Mokni, R., Kherallah, M.: Palmprint identification using glcm texture features extraction and svm classifier. Journal of Information Assurance & Security 11(2) (2016)
30. Mokni, R., Zouari, R., Kherallah, M.: Pre-processing and extraction of the rois steps for palmprints recognition system. Intelligent Systems Design and Applications (ISDA),2015 International Conference on pp. 380–385 (2015)
31. Otsu, N.: A threshold selection method from gray-level histograms. Automatica 11(285-296), 23–27 (1975)
32. Shanmugavadivu, P., Sivakumar, V.: Fractal dimension based texture analysis of digital images. Procedia Engineering 38, 2981–2986 (2012)
33. Simoncelli, E.P., Freeman, W.T.: The steerable pyramid: A flexible architecture for multi-scale derivative computation. In: icip. p. 3444. IEEE (1995)
34. Srivastava, A., Klassen, E., Joshi, S.H., Jermyn, I.H.: Shape analysis of elastic curves in euclidean spaces. IEEE Trans. Pattern Anal. Mach. Intell. 33(7), 1415–1428 (2011)
35. Tan, X., Chen, S., Zhou, Z.H., Zhang, F.: Face recognition from a single image per person: A survey. Pattern recognition 39(9), 1725–1745 (2006)
36. Tunkpien, P., Panduwadeethorn, S., Phimoltares, S.: Compact extraction of principle lines in palmprint using consecutive filtering operations. In: Proceedings of the Second International Conference on Knowledge and Smart Technologies. vol. 2010 (2010)
37. Wang, X., Lei, L., Wang, M.: Palmprint verification based on 2d–gabor wavelet and pulse-coupled neural network. Knowledge-Based Systems 27, 451–455 (2012)
38. Wu, X.Q., Wang, K., Zhang, D.: An approach to line feature representation and matching for palmprint recognition. Journal of Software 15(6), 869–880 (2004)
39. Xia, B., Amor, B.B., Drira, H., Daoudi, M., Ballihi, L.: Combining face averageness and symmetry for 3d-based gender classification. Pattern Recognition 48(3), 746–758 (2015)
40. Zhu, L., Xing, R.: Hierarchical palmprint recognition based on major line feature and dual tree complex wavelet texture feature. In: Fuzzy Systems and Knowledge Discovery, 2009. FSKD'09. Sixth International Conference on. vol. 4, pp. 15–19. IEEE (2009)
41. Zouari, R., Mokni, R., Kherallah, M.: Identification and verification system of offline handwritten signature using fractal approach. In: Image Processing, Applications and Systems Conference (IPAS), 2014 First International. pp. 1–4. IEEE (2014)